Supporting Information:

Atmospheric air plasma treated SnS films: an efficient electrocatalyst for HER

Po-Chia Huang[1], *Sanjaya Brahma*[1], *Po-Yen Liu*[1], *Jow-Lay Huang*[1,2, 3,], *Sheng-Chang Wang*[4,f*], *Shao-Chieh Weng*[1]

[1]Department of Materials Science and Engineering, National Cheng Kung University, Tainan 70101, Taiwan.

[2] Center for Micro/Nano Science and Technology, National Cheng Kung University, Tainan 70101, Taiwan.

[3]Hierarchical Green-Energy Materials (Hi-GEM) Research Center, National Cheng Kung University, Tainan 70101, Taiwan

[4]Department of Mechanical Engineering, Southern Taiwan University of Science and Technology, Tainan 710, Taiwan

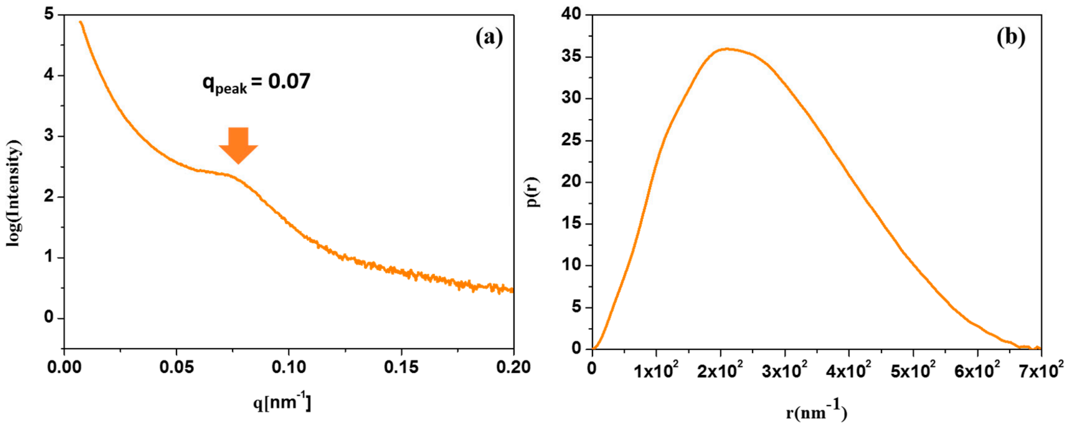

Fig. S1. SAXS radiation of SnS nanocrystals: (a) real data (b) pair distance distribution function (PDDF) data

In Fig. S1 (a) shows the SAXS (small-angle X-ray scattering) radiation of SnS nanocrystals. Particles in an amorphous packing, like particles in a colloidal crystal, are characterized by an average interparticle distance, though the variation around this average distance is greater in amorphous packings than in crystalline ones. The position of the SAXS peak is approximately related to this distance by an equation ($d_{max} = 2\pi \div q_{peak}$), which gives an inter particle distance on the order of the particle diameter for our data. The distance of SnS nanocrystals d_{max} is 9 nm[1].

The generalized indirect Fouier trarnsformation results in p(r) functions that are typical for flat disk objects, with a maximum dimension of 70 nm (as shown in Fig. S1). Compare to literature, the curve display a broad and asymmetry semicircle, which best described by assuming flat disk[2].

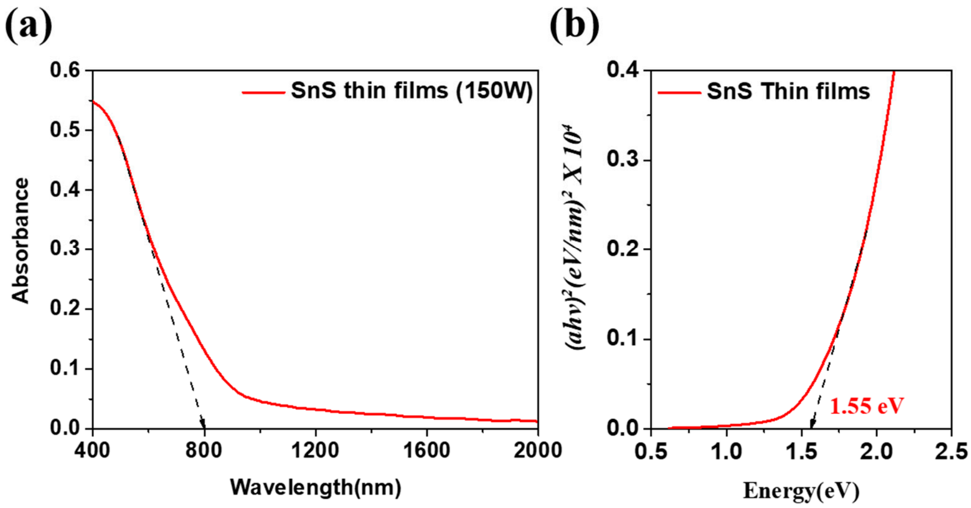

Fig. S2. (a) UV-Vis absorption spectra as a function of incident photon wavelength for SnS thin films after 150W AAPT treatment. (b) Extrapolation of direct bandgap value of SnS thin films after 150W AAPT treatment.

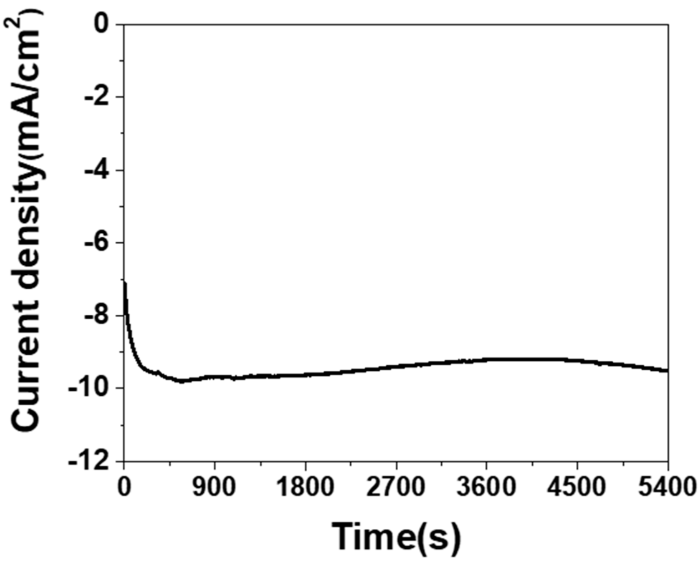

Fig. S3. (a) SnS thin film at -325 mV vs. RHE for 5400 s stabilized test.

Table S1. Literature properties of HER catalysts (as mentioned in the main text)

Single catalyst	Current density (mA/cm^2)	Overpontential (mV, vs RHE)	Tafel value (mV/dec)	Electrolyte	Ref.
MoS_2	N/A	N/A	101.8	0.5 M H_2SO_4	[3]
MoO_2	N/A	N/A	86.4	0.5 M H_2SO_4	[3]
MoS_2	1.42	-300	185	0.5 M H_2SO_4	[4]
WSe_2	10	-98	158	0.5 M H_2SO_4	[5]
Mo_2C	1	-204	87.6	0.1 M $HClO_4$	[6]
WS_2	10	-236	97	0.5 M H_2SO_4	[7]
WS_2	>2.5	400	160	0.5 M H_2SO_4	[8]
FeS_2	10	N/A	56.4	0.5 M H_2SO_4	[9]
CoS_2	10	192	52	0.5 M H_2SO_4	[9]
NiS_2	10	N/A	48.8	0.5 M H_2SO_4	[9]
SnS	>2.5	-600	266	0.5 M H_2SO_4	[10]
SnS	10	-634	174	0.5 M H2SO4	This work
SnS (150W AAPT)	10	-325	60	0.5 M H2SO4	This work
SnS (250W AAPT)	10	-747	210	0.5 M H2SO4	This work
Composite catalyst	Current density (mA/cm^2)	Overpontential (mV, vs RHE)	Tafel value (mV/dec)	Electrolyte	Ref.

MoS_2/MoO_2 on carbon cloth	85	-300	35.6	0.5 M H_2SO_4	[3]
MoS_2/C	14.3	-300	64	0.5 M H_2SO_4	[4]
$W(Se_xS1_{-x})$	10	-174	106	0.5 M H_2SO_4	[5]
Mo_2C/CNT	1	-63	55.2	0.1 M $HClO_4$	[6]
rGO/WS_2	10	-229	73	0.5 M H_2SO_4	[7]
$WS_2/HNCNFs$	10	90	60	0.5 M H_2SO_4	[8]
SnS/N-rGr	10	-125	38	0.5 M H_2SO_4	[10]
MoSx/sponge	71	-200	N/A	0.5 M H_2SO_4	[11]
$MoS_2/TCNQ/$ carbon cloth	51	-200	40	0.5 M H_2SO_4	[12]

REFERENCES

([1] M. Spannuth, S.G.J. Mochrie, S.S.L. Peppin, J.S. Wettlaufer, Particle-scale structure in frozen colloidal suspensions from small-angle x-ray scattering, Phys Rev E, 83 (2011).
[2] D.I. Svergun, M.H.J. Koch, Small-angle scattering studies of biological macromolecules in solution, Rep Prog Phys, 66 (2003) 1735-1782.
[3] R.D. Nikam, A.Y. Lu, P.A. Sonawane, U.R. Kumar, K. Yadav, L.J. Li, Y.T. Chen, Three-Dimensional Heterostructures of MoS2 Nanosheets on Conducting MoO2 as an Efficient Electrocatalyst To Enhance Hydrogen Evolution Reaction, Acs Applied Materials & Interfaces, 7 (2015) 23328-23335.
[4] L. Ma, X.P. Zhou, X.Y. Xu, L.M. Xu, L.L. Zhang, W.X. Chen, One-step hydrothermal synthesis of few-layered and edge-abundant MoS2/C nanocomposites with enhanced electrocatalytic performance for hydrogen evolution reaction, Advanced Powder Technology, 26 (2015) 1273-1280.
[5] M.L. Zou, J.D. Chen, L.F. Xiao, H. Zhu, T.T. Yang, M. Zhang, M.L. Du, WSe2 and W(SexS1-x)(2) nanoflakes grown on carbon nanofibers for the electrocatalytic hydrogen evolution reaction, J Mater Chem A, 3 (2015) 18090-18097.
[6] W.F. Chen, C.H. Wang, K. Sasaki, N. Marinkovic, W. Xu, J.T. Muckerman, Y. Zhu, R.R. Adzic, Highly active and durable nanostructured molybdenum carbide electrocatalysts for hydrogen production, Energ Environ Sci, 6 (2013) 943-951.
[7] T.A. Shifa, F.M. Wang, Z.Z. Cheng, X.Y. Zhan, Z.X. Wang, K.L. Liu, M. Safdar, L.F. Sun, J. He, A vertical-oriented WS2 nanosheet sensitized by graphene: an advanced electrocatalyst for hydrogen evolution reaction, Nanoscale, 7 (2015) 14760-14765.
[8] S. Yu, J. Kim, K.R. Yoon, J.W. Jung, J. Oh, I.D. Kim, Rational Design of Efficient Electrocatalysts for Hydrogen Evolution Reaction: Single Layers of WS2 Nanoplates Anchored to Hollow Nitrogen-Doped Carbon Nanofibers, Acs Applied Materials & Interfaces, 7 (2015) 28116-28121.
[9] M.S. Faber, M.A. Lukowski, Q. Ding, N.S. Kaiser, S. Jin, Earth-Abundant Metal Pyrites (FeS2, CoS2, NiS2, and Their Alloys) for Highly Efficient Hydrogen Evolution and Polysulfide Reduction Electrocatalysis, J Phys Chem C, 118 (2014) 21347-21356.
[10] S.S. Shinde, A. Sami, D.H. Kim, J.H. Lee, Nanostructured SnS-N-doped graphene as an advanced electrocatalyst for the hydrogen evolution reaction, Chem Commun, 51 (2015) 15716-15719.
[11] Y.H. Chang, F.Y. Wu, T.Y. Chen, C.L. Hsu, C.H. Chen, F. Wiryo, K.H. Wei, C.Y. Chiang, L.J. Li, Three- Dimensional Molybdenum Sulfi de Sponges for Electrocatalytic Water Splitting, Small, 10 (2014) 895-900.
[12] Y.H. Chang, R.D. Nikam, C.T. Lin, J.K. Huang, C.C. Tseng, C.L. Hsu, C.C. Cheng, C.Y. Su, L.J. Li, D.H.C. Chua, Enhanced Electrocatalytic Activity of MoSx on TCNQ-Treated Electrode for Hydrogen Evolution Reaction, Acs Applied Materials & Interfaces, 6 (2014) 17679-17685.